Massive Star Formation: Observations confront Theory
ASP Conference Series, Vol. XXX, 2007
H. Beuther et al. (eds.)

Determining the relative evolutionary stages of very young massive star formation regions

S.N.Longmore[1,2,3,7], M.G.Burton[1], C.R.Purcell[4], P.Barnes[5] & J.Ott[6]

Abstract.
We have recently completed an observing program with the Australia Telescope Compact Array towards massive star formation regions traced by 6.7 GHz methanol maser emission. We found the molecular cores could be separated into groups based on their association with/without methanol maser and 24 GHz continuum emission. Analysis of the molecular and ionised gas properties suggested the cores within the groups may be at different evolutionary stages. In this contribution we derive the column densities and temperatures of the cores from the NH_3 emission and investigate if this can be used as an indicator of the relative evolutionary stages of cores in the sample.

The majority of cores are well fit using single-temperature large velocity gradient models, and exhibit a range of temperatures from $\sim$10 K to $>$200 K. Under the simple but reasonable assumption that molecular gas in the cores will heat up and become less quiescent with age due to feedback from the powering source(s), the molecular gas kinetic temperature combined with information of the core kinematics seems a promising probe of relative core age in the earliest evolutionary stages of massive star formation.

1. Introduction

Although short in astronomical terms, the formation time-scale for massive stars is long enough that observations of an individual massive star formation (MSF) region can only provide a snap-shot of the formation process. Given the paucity of young Galactic MSF regions, developing an end-to-end model of the formation process will be greatly facilitated by the ability to accurately determine the relative evolutionary stage of different regions. Observationally, MSF regions tend to be placed into broadly defined groups such as ultra-compact and hyper-compact HII regions and hot/cold molecular cores. However, it is not clear if the discrete nature of the formation process implied by this grouping is a physical

[1]School of Physics, University of New South Wales, Kensington, NSW 2052, Sydney, Australia

[2]Australia Telescope National Facility, CSIRO, PO Box 76, Epping, NSW 1710, Australia

[3]Harvard-Smithsonian Center for Astrophysics, 60 Garden Street, Cambridge, MA 02138, USA

[4]University of Manchester, Jodrell Bank Observatory, Macclesfield, Cheshire SK11 9DL, UK

[5]School of Physics A28, University of Sydney, NSW 2006, Australia

[6]National Radio Astronomy Observatory, 520 Edgemont Road, Charlottesville, VA 22903, USA

[7]E-mail: slongmore@cfa.harvard.edu

reality (suggesting each of currently defined groups represent relatively long-lived stages which quickly transition to the next stage), or if the formation process is in fact more continuous.

In an attempt to develop our understanding of the early evolutionary stages of the MSF process, Longmore et al. (2007a) (L07A) have completed an observing program with the Australia Telescope Compact Array (ATCA) towards MSF regions traced by 6.7 GHz methanol maser emission (a powerful sign-post of very early massive star formation). The aim of these observations was to derive the physical properties of the gas in these regions and see how accurately it is possible to determine the relative evolutionary stages of the cores. The initial results suggested cores could be separated into different evolutionary stages based on their association with/without methanol maser and 24 GHz continuum emission. In this contribution we focus on deriving the core temperatures and investigate the use of molecular gas kinetic temperature as an indicator of the cores' evolutionary stage.

2. Deriving properties of molecular gas from NH_3 observations

2.1. Observations

Observations of NH_3(1,1), (2,2), (4,4) & (5,5) and 24 GHz continuum were carried out using the ATCA towards 21 MSF regions traced by 6.7 GHz methanol maser emission. The H168 [NH_3(1,1) & (2,2) observed simultaneously] and H214 [NH_3(4,4) & (5,5) observed simultaneously] antenna configurations with both East-West and North-South baselines, were used to allow for snapshot imaging. Primary and characteristic synthesised beam sizes were $\sim 2.'2$ and $\sim 8 - 11''$ respectively. Characteristic spectra were extracted at every transition for each core at the position of the peak NH_3(1,1) emission and fit using CLASS. The NH_3 column density and gas kinetic temperature were calculated from the L07A data using the standard analysis procedure (see e.g. Ho & Townes 1983; Ungerechts et al. 1986). In § 2.2., we assess the validity of the assumptions used in this procedure for the L07A sample. § 2.3. outlines the large velocity gradient models used to derive gas kinetic temperatures.

2.2. Assessing the assumptions used in the standard NH_3 analysis

The three main underlying assumptions in the standard analysis used to derive NH_3 column density and molecular gas kinetic temperature are that:

1. the excitation temperature is the same for all hyperfine components within an inversion transition.

2. the excitation temperature is the same for all inversion transitions.

3. the emission from all inversion transitions comes from the same gas so has equal line width and beam filling factor.

The validity of these assumptions for the L07A data are assessed below.

Assumption 1 Given the extreme $NH_3(1,1)$ hyperfine anomalies in the outer satellite lines of some L07A spectra, the first assumption is clearly invalid for these outer satellites. The optical depth derived from CLASS (which fits to all 18 components under the equal excitation temperature assumption) is therefore potentially incorrect. As hyperfine structure is not detected in the other inversion transitions, it is not possible to check for further anomalies in the excitation conditions.

Assumption 2 Without detected hyperfine structure in the energy levels above $NH_3(1,1)$, it is not possible to measure the excitation temperature within other inversion transitions to test the second assumption. Given the very similar morphology of the $NH_3(1,1)$ and (2,2) emission, this lends support to the idea that the excitation conditions are similar for these two transitions. However, the same cannot be said for the $NH_3(4,4)$ & (5,5) emission [as this is always unresolved], rendering the second assumption suspect for these cores.

Assumption 3 As the $NH_3(1,1)$ and (2,2) emission is generally somewhat extended with very similar morphology, the assumption that emission in these transitions is from the same gas seems valid. However, as the $NH_3(4,4)$ & (5,5) emission is always unresolved, it is not possible to test this assumption for these transitions.

In summary, the standard analysis:

- will be reliable for sources detected only in $NH_3(1,1)$ and (2,2) with no $NH_3(1,1)$ hyperfine anomalies
- will introduce an uncertainty in the derived optical depth for sources detected in only $NH_3(1,1)$ and (2,2) with $NH_3(1,1)$ hyperfine anomalies
- may not be reliable for sources with detected $NH_3(4,4)$ and (5,5) emission. Modelling is required to derive accurate properties of the gas for these sources.

2.3. LVG modelling

Having derived a column density for each detected transitions for all the cores, we used the large velocity gradient (LVG) models described in Ott et al. 2005 to derive the core kinetic temperatures. Assuming a velocity gradient of 1 $\mathrm{kms^{-1}pc^{-1}}$, background temperature of 2.73 K and hydrogen volume density of $10^5\mathrm{cm^{-3}}$, χ^2 minimisation was used to calculate the best-fit kinetic temperature and total ammonia column density to the measured column density within each transition.

3. Results

Column Density Figure 1 shows the histogram of the total NH_3 column density derived using the standard NH_3 analysis procedure. The mean value of $\sim 10^{15}\,\mathrm{cm^{-2}}$ is similar to values derived for other high-mass cores.

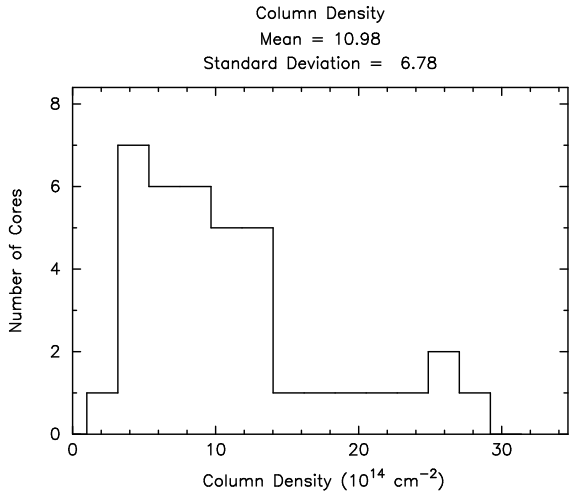

Figure 1. Histogram of the total NH_3 column density.

Temperature Figure 2 shows a temperature histogram for cores with only detected NH_3(1,1) & (2,2) emission (for which the assumptions in the standard analysis should be reliable). Given that this includes cores with large NH_3(1,1) hyperfine anomalies (potentially introducing uncertainties in the NH_3(1,1) column density and hence temperature), the spread in temperature for these cores is relatively small.

The temperature derivation for cores with detected NH_3(4,4) & (5,5) emission is more complicated. The single-temperature LVG model fits well to most cores but poorly to others. To illustrate this, Figure 3 shows rotational diagrams (effectively column density within each transition vs. transition energy) for three example cores, with the best-fit temperature plotted as a straight line. Both of the cores in the top [only detected at NH_3(1,1) & (2,2)] and middle plots are well fit with a single temperature component. Conversely, the column densities calculated for the core in the bottom plot are clearly poorly fit with a single temperature component. However, as described in § 2.1., the NH_3(1,1) & (2,2) transitions were observed using a different array configuration and set-up to the NH_3(4,4) & (5,5) transitions. It is therefore possible that the bad fit to a single temperature component is an artefact of comparing gas properties derived from the different observing set-ups. Firstly, comparing column densities between these two line pairs may suffer from systematic offsets caused by the $\sim$10% uncertainty in the absolute flux calibration that doesn't affect the simultaneously observed line-pairs. Similarly, the slightly different array configurations used to observe the two line-pairs may be introducing an offset in the derived column densities as each observation samples slightly different spatial structure. However, as each of the line-pairs were observed simultaneously, they sample the same spatial structure and have the same absolute flux calibration error. As the temperature between two transitions is calculated from the ratio of measured intensity (rather than the absolute intensity used to derive the column density) temperatures derived between NH_3(1,1) & (2,2) [T_{12}] and NH_3(4,4) &

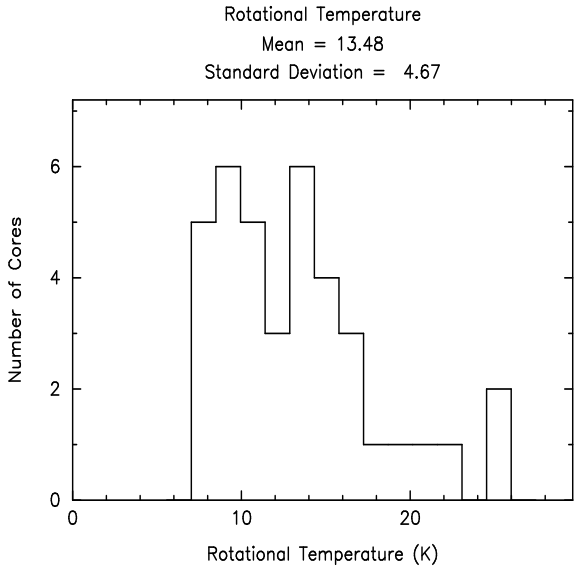

Figure 2. Histograms of the molecular gas temperature derived from the cores with NH_3(1,1) & (2,2) emission.

(5,5) [T_{45}] will not suffer these problems. Additionally, the line-pairs have similar excitation temperatures (23 & 64 K vs 200 & 295 K for NH_3(1,1) & (2,2) vs NH_3(4,4) & (5,5), respectively) so are much more likely to be sampling the same gas. Deriving temperatures for these line-pairs suggests there are two seperate components – a cold component traced by T_{12} and a hot component traced by T_{45}. Comparing the observed morphology of the line-pairs (the NH_3(4,4) & (5,5) emission always being unresolved at the central peak of the generally extended NH_3(1,1) & (2,2) emission) further points to the emission from these line-pairs coming from different gas. If so, this renders assumptions 2 and 3 in §2.2. (used to derive the NH_3(4,4) & (5,5) column densities) invalid. In conclusion, while it seems likely there are multiple temperature components in these cores, further analysis (e.g. radiative transfer modelling to fit the physical structure of the core to the observed spectra) is required to determine how this relates to the core structure. Therefore, in the remaining sections we limit ourselves to discussing the general spread in the core temperatures rather than focusing on individual temperature measurements themselves.

4. Discussion

Analysis of the molecular/ionised gas in L07A suggested cores grouped according to their association with/without 6.7 GHz methanol maser and 24 GHz continuum emission were potentially at different evolutionary stages. Making the reasonable assumption that cores heat up and becomes less quiescent with age, we now investigate how the derived molecular gas temperature fits in with the proposed evolutionary scenario. As the core sizes are similar, L07A used the

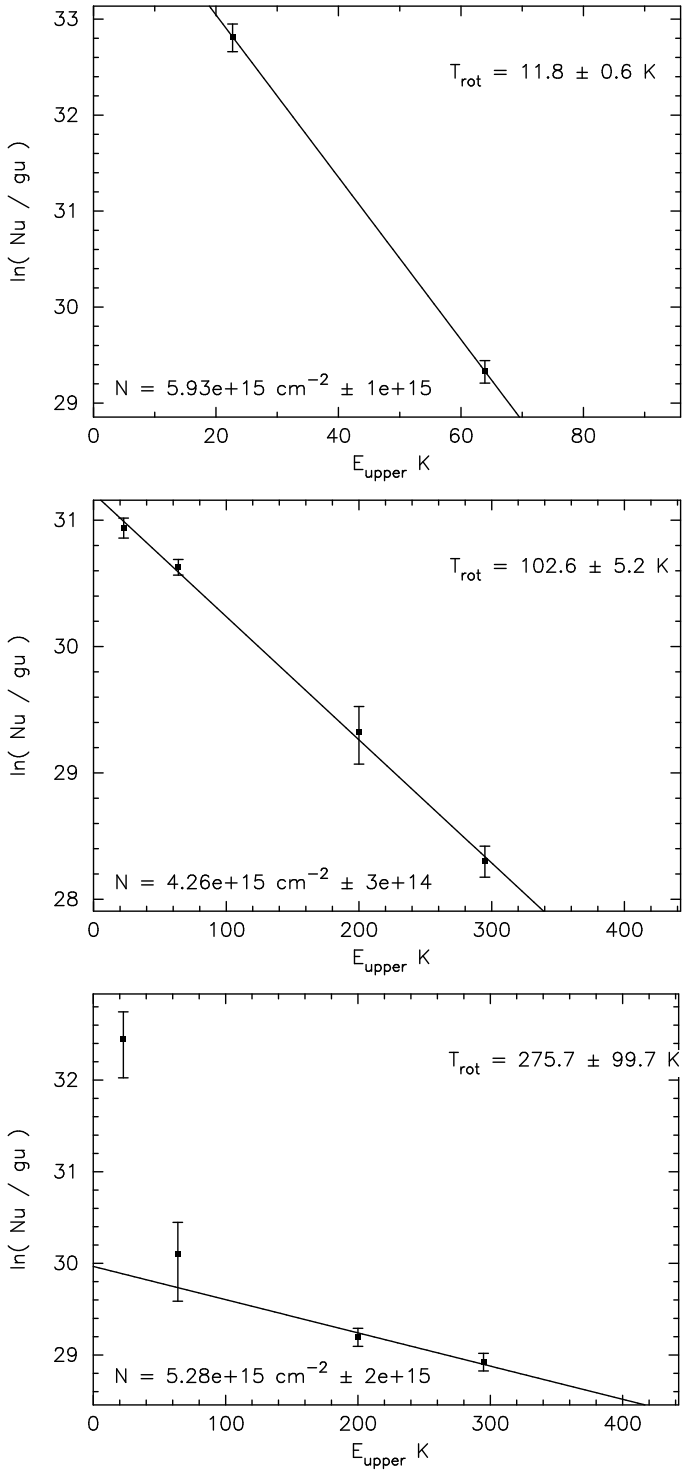

Figure 3. Example NH_3 rotational diagrams for three cores, plotting the column density derived for each transition as a function of the transition energy. The straight line shows the weighted best-fit line through the points. The temperature is proportional to the inverse of the line gradient (the value of which is shown in the top-right of each plot) and the intercept point on the y-axis gives the total NH_3 column density (the value of which is shown in the bottom-left of each plot). The core in the top plot is only detected at $NH_3(1,1)$ & (2,2) while the cores in the middle and bottom plot are detected from $NH_3(1,1) \rightarrow (5,5)$. The cores in the top and middle plots are well fit by a single temperature model but the single temperature approximation is

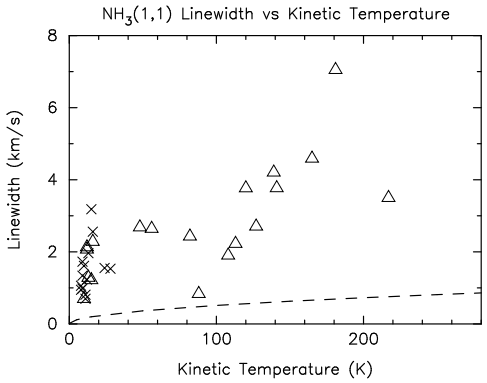

Figure 4. $NH_3(1,1)$ linewidth vs gas kinetic temperature. Cores with NH_3 emission only (Group 1 in L07A) are shown as crosses while those with NH_3 and methanol maser emission (Groups 2 and 3 in L07A) are shown as triangles. The dashed line shows the expected linewidth due to purely thermal motions.

$NH_3(1,1)$ linewidths as a reliable indicator of how quiescent the gas is, without worrying about its dependence on the core size (Larson 1981). Figure 4 [from Longmore et al. (2007b)] shows $NH_3(1,1)$ core linewidth vs kinetic temperature. Triangles and crosses show sources with/without methanol maser emission, respectively. The molecular gas in sources with methanol maser emission (triangles) are generally significantly warmer than those without (crosses). However, there are also a small number of cores with methanol maser emission that have very cool temperatures and quiescent gas, similar to the NH_3-only cores. Modelling shows pumping of 6.7 GHz methanol masers requires local temperatures sufficient to evaporate methanol from the dust grains (T>$\sim$90K) and a highly luminous source of IR photons [Cragg et al. (2005)] i.e. an internal powering source. It is therefore plausible that the cold, quiescent sources with methanol maser emission are cores in which the feedback from the powering sources have not had time to significantly alter the larger scale properties of the gas in the cores. It is worth noting that Krumholz (2006) predicts accretion luminosity at the earliest stages of core collapse can heat the inner regions to 100 K. This would raise the characteristic fragmentation mass above that in the outer regions, effectively suppressing fragmentation in the inner regions. The sources we observe with potentially more than one temperature component are therefore interesting targets for testing the competitive accretion vs. turbulent core models of the formation process.

Finally, concentrating on cores with a well defined temperature, we note that: 1) there are a large number of cold (10 to 20 K) cores with quiescent gas which may be regions at the very earliest evolutionary stages before any star-formation feedback has effected the natal molecular material, and 2) the spread in core temperature from $\sim$20 to 200 K is continuous, suggesting the transition from 'cold' to 'hot' core is not discrete. This urges a note of caution when comparing samples of hot and cold cores or assuming a single dust temperature when deriving properties for numerous sources from mm continuum emission.

5. Conclusions

Based on the NH_3 observations of Longmore et al. (2007a), we have performed a preliminary analysis of core temperature towards a sample of very young MSF regions, to try and determine their relative evolutionary stages. We find,

- a large number of cold ($\sim 10\,K$) cores with very quiescent gas. These are likely to be MSF regions at the earliest evolutionary stages.
- above $\sim$20 K the cores exhibit a smooth range in temperature suggesting the transition from 'cold' to 'hot' cores is continuous rather than discrete.
- two lines of evidence suggesting some of the cores have more than one temperature component. Although more detailed modelling is required to accurately derive the core structure, these are potentially interesting for future study as regions in which the central powering sources has only recently begun to heat up its surrounding environment.

In summary, molecular gas kinetic temperature combined with information of the core kinematics appears to be a promising way to compare the evolutionary state of very young MSF regions.

Acknowledgments. We would like to thank Thushara Pillai for her instructive comments. SNL acknowledges support through a School of Physics scholarship at UNSW. The Australia Telescope is funded by the Commonwealth of Australia for operation as a National Facility managed by CSIRO. This research has made use of NASA's Astrophysics Data System. We also thank the Australian Research Council for funding support from grant number DP0451893.

References

Cragg D. M., Sobolev A. M., Godfrey P. D., 2005, MNRAS, 360, 533
Ho P. T. P., Townes C. H., 1983, ARA&A, 21, 239
Krumholz M. R., 2006, ApJ, 641, L45
Larson R. B., 1981, MNRAS, 194, 809
Longmore S. N., Burton M. G., Barnes P. J., Wong T., Purcell C. R., Ott J., 2007a, MNRAS, 379, 535
Longmore S. N., Burton M. G., Barnes P. J., Wong T., Purcell C. R., Ott J., 2007b, in Baan W., Chapman J., eds, IAU Symposium 242, Astrophysical masers and their environments, The molecular environment of massive star forming cores associated with Class II methanol maser emission
Ungerechts H., Winnewisser G., Walmsley C. M., 1986, A&A, 157, 207